

ESTIMATE FAILURE PROBABILITY WITH NEURAL OPERATOR HYBIRD APPROACH *

MUJING LI [†], YANI FENG [‡], AND GUANJIE WANG [§]

Abstract. The evaluation of failure probability for complex engineering system is a computationally intensive task. While the Monte Carlo method is easy to implement, it converges slowly and therefore requires numerous repeated simulations of the failure model to generate sufficient samples. To improve the efficiency, methods based on surrogate models are proposed to approximate the limit state function. In this work, we reframe the approximation of the limit state function as an operator learning problem and utilize the DeepONet framework with a hybrid approach to estimate the failure probability. Numerical results show that our proposed method outperforms the prior neural hybrid method.

Key words. failure probability; neural operator learning; DeepONet; approximation theory

AMS subject classifications. 68Q25, 68R10, 68U05

1. Introduction. In practice, the evaluation of failure probability for systems that inherently contain uncertainty is a fundamental problem encountered in various fields, such as structural safety, risk management, and reliability-based optimization. While the mathematical formulation of the problem is well-defined, evaluating the multivariate integrals over the domains defined by failure models remains a challenging task in practice.

The most straightforward approach to evaluate the failure probability is to use the Monte Carlo sampling (MCS) method [1, 8]. However, due to its slow convergence, MCS requires numerous samples, resulting in a heavy computational burden. This computational burden becomes even more pronounced when complex stochastic PDEs are used to represent the failure models, since MCS necessitates repeatedly solving the model to estimate the failure probability.

To address this issue, various approaches have been developed, including the first-order reliability method (FORM) [7], second-order method (SORM) [11], and response surface method (RSM) [31, 13]. These methods replace the failure model with a surrogate model that is easy to evaluate, thereby greatly reducing the simulation time. Following this idea, the hybrid method was proposed by [17, 16], which estimates the probability based on the surrogate model while re-evaluating samples in a given suspicious region. The design of the hybrid method significantly reduces the time complexity while ensuring accuracy.

There are various methodologies for constructing surrogate models, such as the stochastic Galerkin method [10, 34], the reduced basis method [2, 29], and deep learning. In recent decades, deep learning has rapidly developed, particularly in scientific

*Submitted to the editors DATE.

Funding: M. Li and Y. Feng are supported by the National Natural Science Foundation of China (No. 12071291), the Science and Technology Commission of Shanghai Municipality (No. 20JC1414300), and the Natural Science Foundation of Shanghai (No. 20ZR1436200). G. Wang is supported by the Colleges and Universities Young Teachers Training and Funding Program of Shanghai (No. ZZLX21039)

[†]School of Information Science and Technology, ShanghaiTech University, Shanghai 201210, P. R. China (limj@shanghaitech.edu.cn).

[‡]School of Information Science and Technology, ShanghaiTech University, Shanghai 201210, P. R. China (fengyn@shanghaitech.edu.cn).

[§]School of Statistics and Mathematics, Shanghai Lixin University of Accounting and Finance, 201209, Shanghai, P. R. China (guanjie@lixin.edu.cn).

and engineering applications. Physics-informed neural networks (PINNs), which build upon the widely known universal approximation capability of continuous functions for neural networks (NN) [6, 12], are introduced in [30] and have demonstrated their efficiency in numerous studies [24, 26, 36]. By utilizing established deep learning and machine learning techniques, NN models can be employed as surrogate models to approximate the limit state function, outperforming traditional surrogate models in certain problem like high-dimensional systems [18, 20, 35].

The operator learning, which is based on the fact that single-layer neural networks can approximate any nonlinear operator [4, 5] (Theorem 3.1, aims to map infinite-dimensional functions to infinite-dimensional functions. Since it is more expressive and can break the curse of dimensionality in input space [23], the operator learning has gained a lot of attentions in recent years [23, 19, 22]. Among the operator learning techniques, the DeepONet introduced in [22, 23], has demonstrated its effectiveness in numerous applications, including [21, 3, 25].

In this work, we present a novel approach for the failure probability estimation by reframing the approximation problem of the limit state function as an operator learning problem, and subsequently adapting the DeepONet framework to address it. The operator learning formulation provides a more effective and generalized approach to constructing a surrogate model for the limit state function, resulting in enhanced precision and reduced simulation numbers. To further expedite the algorithm, we employ a hybrid method [17] for estimating the failure probability. Our proposed neural operator hybrid (NOH) approach significantly reduces time complexity while maintaining high accuracy compared to earlier neural surrogate and Monte Carlo simulation approaches. We posit that the efficiency of our approach in estimating failure probability demonstrates the potential of operator learning in various tasks.

The paper is structured as follows: In Section 2, we present the problem setting and introduce a hybrid method for evaluating the failure probability. The Neural operator learning and proposed algorithm is then fully described in Subsection 3.2. To demonstrate the effectiveness of our approach, we conduct numerical experiments in Section 4, covering a variety of scenarios, including ODEs, PDEs, and multivariate models. Finally, we offer concluding remarks and observations in Section 5.

2. Preliminaries. This section will provide an overview of the mathematical framework for failure probability and introduce a hybrid method for solving this problem.

2.1. Problem setting. Let $Z = (Z_1, Z_2, \dots, Z_{n_z})$ be an n_z -dimensional random vector with distribution function $F_Z(z) = \text{Prob}(Z \leq z)$. The image of Z , i.e., the set of all possible values that Z can take, is denoted by Ω . It is our interest to evaluate the failure probability P_f defined by:

$$(2.1) \quad P_f = \text{Prob}(Z \in \Omega_f) = \int_{\Omega_f} dF_Z(z) = \int \chi_{\Omega_f}(z) dF_Z(z) = E[\chi_{\Omega_f}(z)],$$

where the characteristic function $\chi_{\Omega_f}(z)$ is defined as:

$$(2.2) \quad \chi_{\Omega_f}(z) = \begin{cases} 1 & \text{if } z \in \Omega_f, \\ 0 & \text{if } z \notin \Omega_f, \end{cases}$$

and the failure domain Ω_f , where failure occurs, is defined as:

$$(2.3) \quad \Omega_f = \{Z : g(Z) < 0\}.$$

Here, $g(Z)$ is a scalar limit state function, also known as a performance function, that characterizes the failure domain. It should be emphasized that, in many real-world systems, $g(Z)$ does not have an analytical expression and is instead characterized by a complex system that requires simulations to evaluate. Consequently, the evaluation of $g(Z)$ can be computationally expensive, leading to significant time complexity in the algorithm.

2.2. Hybrid Method. The most straightforward approach to estimate the failure probability is the Monte Carlo sampling (MCS) method [1, 8], given by:

$$(2.4) \quad P_f^{mc} = \frac{1}{M} \sum_{i=1}^M \chi_{\{g(z) < 0\}} \left(z^{(i)} \right),$$

where $\{z^{(i)}\}_{i=1}^M$ is a set of sample points for the random vector Z . The characteristic function $\chi_{\{g(z) < 0\}}(z^{(i)})$ takes a value of 1 if the limit state function $g(Z)$ evaluated at $z^{(i)}$ is less than zero, and 0 otherwise. The failure probability P_f is estimated as the average of the characteristic function over the M sample points.

However, evaluating the limit state function $g(Z)$ at numerous sample points can be a computationally intensive task, especially when dealing with complex stochastic system, which can result in significant simulation time complexity. To address this issue, a surrogate model can be used to approximate the limit state function $g(Z)$ and avoid the need for direct evaluation at each sample point. Specifically, a surrogate model of $g(Z)$ is denoted by $\hat{g}(Z)$ that can be rapidly evaluated. The failure probability can then be estimated as:

$$(2.5) \quad \hat{P}_f^{mc} = \frac{1}{M} \sum_{i=1}^M \chi_{\{\hat{g}(z) < 0\}} \left(z^{(i)} \right).$$

While surrogate models can significantly reduce computational costs in Monte Carlo methods, relying solely on them for estimating the failure probability may result in poor precision or even failure. To address this issue, a hybrid approach that combines sampling of the surrogate models \hat{g} and the limit state function g is proposed in [17, 16]. In the following, we give a brief review of the hybrid method.

Suppose that $(-\gamma, \gamma)$ is a suspicious region, where γ is a non-negative real number. In this case, we can approximate the failure domain Ω_f by $\tilde{\Omega}_f$ as follows:

$$(2.6) \quad \tilde{\Omega}_f = \{\hat{g}(Z) < -\gamma\} \cup \left\{ \{|\hat{g}(Z)| \leq \gamma\} \cap \{g(Z) < 0\} \right\},$$

where g is the limit state function, and \hat{g} represents the surrogate model of g . Enhanced with hybrid method, the failure probability can be estimable by MCS:

$$(2.7) \quad \begin{aligned} P_f^h &= \frac{1}{M} \sum_{i=1}^M \chi_{\tilde{\Omega}_f} \left(z^{(i)} \right), \\ &= \frac{1}{M} \sum_{i=1}^M \left[\chi_{\{\hat{g} < -\gamma\}} \left(z^{(i)} \right) + \chi_{\{|\hat{g}| \leq \gamma\}} \left(z^{(i)} \right) \cdot \chi_{\{g < 0\}} \left(z^{(i)} \right) \right]. \end{aligned}$$

The hybrid method can be considered as an approach for estimating P_f using a surrogate \hat{g} , followed by re-evaluation of the samples within the suspicious domain.

While increasing the value of γ leads to higher time complexity, it also results in more accurate estimation. In [17], it is proved that for any surrogate $\hat{g}(Z)$ and for all $\epsilon > 0$, there exists a critical value $\gamma_N > 0$ such that for all $\gamma > \gamma_N$, the difference between the estimated P_f^h and the truth P_f is less than ϵ , i.e.,

$$(2.8) \quad |P_f - P_f^h| < \epsilon.$$

To be more precisely,

$$(2.9) \quad \gamma_N = \frac{1}{\epsilon^{1/p}} \|g(Z) - \hat{g}(Z)\|_{L_\Omega^p},$$

where the approximation is measured in L^p -norm with $p \geq 1$.

$$(2.10) \quad \|g(Z) - \hat{g}(Z)\|_{L_\Omega^p} = \left(\int_\Omega |g(z) - \hat{g}(z)|^p dF_Z(z) \right)^{1/p}.$$

Selecting an appropriate value of γ that balances accuracy and computational efficiency can be a challenging task. To address this challenge, an iterative algorithm, as demonstrated in Algorithm 2.1, is commonly employed in practice instead of directly selecting γ . In Algorithm 2.1, the surrogate \hat{g} samples are gradually replaced with g samples in the iteration procedure until either the stopping criterion is reached, or when the iteration step reaches $\lceil M/\delta M \rceil$, which is equivalent to expanding the suspicious region at each iteration. When k reaches $\lceil M/\delta M \rceil$, the iterative hybrid algorithm degenerates to the Monte Carlo method (2.4), indicating that the convergence is achieved as $P_f^{(k)} \rightarrow P_f^{mc}$, $k \rightarrow \lceil M/\delta M \rceil$. It is obvious that the time complexity of the iterative hybrid algorithm is heavily influenced by the accuracy of the surrogate model used in Algorithm 2.1.

Algorithm 2.1 Iterative Hybrid Method [17]

Require: surrogate model \hat{g} , $S = \{z^{(i)}\}_{i=1}^M$ samples from random variable Z , tolerance ϵ and sample size in each iteration δM .
 Initialization: $k = 0$.
 Compute $P_f^{(0)} = \frac{1}{M} \sum_{i=1}^M \chi_{\{\hat{g}(z) < 0\}}(z^{(i)})$.
 Sort $\{|\hat{g}(z^{(i)})|\}_{i=1}^M$ in ascending order, sort the correspond sample S accordingly.
for k from 1 to $\lceil M/\delta M \rceil$ **do**
 $\delta S^k = \{z^{(j)}\}_{j=(k-1)\delta M+1}^{k\delta M}$.
 $\delta P = \frac{1}{M} \sum_{z^{(j)} \in \delta S^k} [-\chi_{\{\hat{g} < 0\}}(z^{(j)}) + \chi_{\{g < 0\}}(z^{(j)})]$.
 $P_f^{(k)} = P_f^{(k-1)} + \delta P$.
 if $|\delta P| \leq \epsilon$ for several times **then**
 break
 end if
end for
Ensure: $P_f^{(k)}$

3. Neural Operator Hybrid Algorithm. In Section 2, we describe the failure probability problems and the hybrid algorithm for solving it. As we have mentioned, the accuracy of the surrogate model greatly affects the performance of the iterative

hybrid algorithm. In this section, we introduce the neural operator learning and present the Neural Operator Hybrid (NOH) Algorithm, which reframes the approximation problem of the limit state function as an operator learning problem. Unlike prior studies that use neural networks as surrogate models for linear mappings (as in [18, 20, 35, 27, 15]), our algorithm constructs a surrogate model using operator learning techniques, resulting in a more effective and generalized approach to estimating failure probability.

3.1. Neural Operator Learning. The neural operator learning aims to accurately represent linear and nonlinear operators that map input functions into output functions. More specifically, let U be a vector space of functions on set K_1 , and let V be a vector space of functions on set K_2 , G is an operator map from U to V , i.e.,

$$(3.1) \quad G : u \mapsto G(u) \in V, \text{ for } u \in U,$$

where u is a function defined on the domain K_1 , i.e.,

$$(3.2) \quad u : x \mapsto u(x) \in \mathbb{R}, \text{ for } x \in K_1,$$

and $G(u)$ is a function defined on the domain K_2 , i.e.,

$$(3.3) \quad G(u) : y \mapsto G(u)(y) \in \mathbb{R}, \text{ for } y \in K_1.$$

In the context of this paper, U is referred to as the input function space, and V is referred to as the output function space. It is of interest to design neural networks that can approximate the operator G mapping from the input function space to the output function space.

In this work, we employ the DeepONet framework [22], an up-rising operator learning approach based on the following theorem, to construct the surrogate of the operator G .

THEOREM 3.1 (Universal Approximation Theorem for Operator [5]). *Suppose that σ is a continuous non-polynomial function, X is a Banach Space, $K_1 \subset X, K_2 \subset \mathbb{R}^d$ are two compact sets in X and \mathbb{R}^d , respectively, U is a compact set in $C(K_1)$, G is a nonlinear continuous operator, which maps U into $C(K_2)$. Then for any $\epsilon > 0$, there are positive integers n, p, m , constants $c_i^k, \xi_{ij}^k, \theta_i^k, \zeta_k \in \mathbb{R}, w_k \in \mathbb{R}^d, x_j \in K_1, i = 1, \dots, n, k = 1, \dots, p, j = 1, \dots, m$, such that*

$$|G(u)(y) - \underbrace{\sum_{k=1}^p \sum_{i=1}^n c_i^k \sigma \left(\sum_{j=1}^m \xi_{ij}^k u(x_j) + \theta_i^k \right)}_{\text{branch}} \underbrace{\sigma(w_k \cdot y + \zeta_k)}_{\text{trunk}}| < \epsilon$$

holds for all $u \in U$ and $y \in K_2$.

In DeepONet, the operator G is approximated by taking the inner product of two components, which can be expressed as follows:

$$(3.4) \quad G(u)(y) \approx \mathcal{G}(u)(y) := \sum_{k=1}^p \underbrace{b_k(u)}_{\text{branch}} \underbrace{t_k(y)}_{\text{trunk}},$$

where $b_k(u)$ is the output of the trunk network for a given input function u in U , and $t_k(y)$ is the output of the branch network for a given y in K_2 . Figure 1 illustrates this architecture.

In practical applications, the input function u is vectorized as $[u(x_1), \dots, u(x_m)]^T$, where the sample points $[x_1, x_2, \dots, x_m]^T$ are referred to as **sensors**. The input of trunk network takes P specific value y_1, \dots, y_P in K_2 . The neural network can be trained using the training data

$$(3.5) \quad \mathcal{T} = \left\{ \left(u^{(1)}, G(u^{(1)}) \right), \left(u^{(2)}, G(u^{(2)}) \right), \dots, \left(u^{(N)}, G(u^{(N)}) \right) \right\},$$

and by minimizing the following loss function,

$$(3.6) \quad \mathcal{L}(\Theta) = \frac{1}{N * P} \sum_{l=1}^P \sum_{i=1}^N \|G_{\Theta}(u^{(i)})(y_l^{(i)}) - G(u^{(i)})(y_l^{(i)})\|_2,$$

where the neural network G_{Θ} with parameters Θ approximates the operator G .

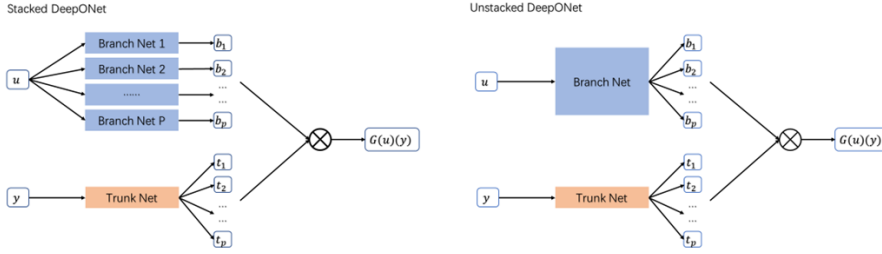


Fig. 1: Illustrations of Stacked and unstacked architectures of DeepONets [22]. Unstacked structure DeepONets replace branch networks with a single multi-layer neural network.

3.2. Neural Operator Hybrid Algorithm. Neural operator learning involves functions as both inputs and outputs, requiring us to reframe our problem accordingly. Let U be the collection of all functions defined on $[0, 1]$ such that

$$(3.7) \quad u(x) = \bar{Z} - k\bar{\sigma} + 2k\bar{\sigma}x, \text{ for } x \in [0, 1],$$

where k is a selective parameter and \bar{Z} and $\bar{\sigma}$ are defined as:

$$(3.8) \quad \bar{Z} = \frac{Z_1 + \dots + Z_{n_z}}{n_z}, \quad \bar{\sigma} = \frac{\sigma_1 + \dots + \sigma_{n_z}}{n_z}.$$

Here $\sigma_1, \dots, \sigma_{n_z}$ are the variance of Z_1, \dots, Z_{n_z} respectively. We can then define an operator G from U to V as follows:

$$G : u \mapsto G(u) \in V, \text{ for } u \in U,$$

where $V = \text{span}\{g(x)\}$ and $G(u)$ is defined by

$$(3.9) \quad G(u) : y \mapsto g(y) \in \mathbb{R}, \text{ for } y \in \mathbb{R}^{n_z}.$$

Here g is the limit state function discussed in Subsection 2.1. Then, designing a surrogate model for G is a standard operator learning problem.

The inspiration for this reframing is to establish a relationship between the input function $u(x)$ and the random variable Z . It is important to note that the prior distribution of $u(x)$ is entirely known, which enables us to generate training data using the following process: Firstly, we sample $z^{(i)}$ randomly according to the random distribution Z , where $i = 1, \dots, N$. Next, we define $u^{(i)}(x)$ using the following equation:

$$(3.10) \quad u^{(i)}(x) = \bar{z}^{(i)} - k\bar{\sigma} + 2k\bar{\sigma}x, \quad x \in [0, 1],$$

where

$$(3.11) \quad \bar{z}^{(i)} = \frac{z_1^{(i)} + \dots + z_{n_z}^{(i)}}{n_z}.$$

In practical implementation, we vectorize the input function $u^{(i)}(x)$ on a uniform grid of the interval $[0, 1]$. Specifically, the vectorized input function is given by $[u^{(i)}(x_1), \dots, u^{(i)}(x_m)]$, where x_j denotes the j -th sensor and is defined by

$$(3.12) \quad x_j = \frac{j-1}{m-1}, \quad j = 1, \dots, m.$$

Suppose that there are P observations $y_l \in \mathbb{R}^{n_z}$, $l = 1, \dots, P$, then by equation (3.9), we have $G(u^{(i)})(y_l) = g(y_l)$. Once the data set is generated, the model is trained by minimizing the following loss function:

$$(3.13) \quad \mathcal{L}(\Theta) = \frac{1}{N * P} \sum_{l=1}^P \sum_{i=1}^N \|G_{\Theta}(u^{(i)})(y_l) - g(y_l)\|_2,$$

where G_{Θ} is a neural network with parameters Θ that approximates the operator G . Here, $\{u^{(i)}\}_{i=1}^N$ denotes different input functions and $\{y_l\}_{l=1}^P$ are P locations from data observations for each $G(u^{(i)})$.

After constructing the surrogate for G using the neural network G_{Θ} , we can integrate it into a hybrid algorithm to estimate the failure probability. This entire process is named the Neural Operator Hybrid (NOH) method.

As discussed in Subsection 2.2, the convergence of Algorithm 2.1 $|P_f - P_f^h| < \epsilon$ is dependent on the norm measurement of the surrogate and the limit state function, i.e., $|g(Z) - \hat{g}(Z)|$. An accurate approximation $\hat{g}(Z)$ is essential for reliable estimation, which is ensured by Theorem 3.1 for DeepONet. Additionally, DeepONet exhibits less generalization error [22] than simple neural networks, given explanation to better performance in numerical experiments.

Our goal is to demonstrate the difference between the NOH and Neural Hybrid (NH) methods, which employed neural surrogate in hybrid method, and show that by reformulating the problem into an operator learning framework and designing an appropriate neural network structure, we can achieve significant performance improvements. While techniques such as importance sampling (IS) [16, 32] or adaptive learning [20, 33] can further reduce the required sample size. We aim to compare our approach to previous work [18], so only the vanilla hybrid method with different surrogate models is used. These techniques can be employed for further improvement in future work.

4. Numerical experiment. In this section, we present three numerical examples to demonstrate the efficiency and effectiveness of the proposed Neural Operator Hybrid (NOH) method. Furthermore, we compare the NOH method with the Neural Hybrid (NH) method, where the limit state function g is approximated using a neural surrogate constructed by the classical neural networks. For the purpose of clarity in presentation, we refer to the surrogate constructed using classical neural networks for g in the NH method as **the neural surrogate**, and the surrogate constructed using DeepONet for G in the NOH method as **the neural operator surrogate**.

For the NOH method, we use the simplest unstacked DeepONet to construct the neural operator surrogate for the operator G , with the branch and trunk networks implemented as fully connected neural networks (FNNs). The trunk network is employed with a depth of 2 and a width of 40 FNN, while the branch network has a depth of 2 and a width of 40 FNN. To facilitate a comparative analysis with the NH method, we built a neural surrogate for g using a simple FNN with a parameter size comparable to that of the NOH method. Specifically, in the NH method, the FNN utilized for the neural surrogate has a depth of 3, and its width is adjusted to achieve a similar number of parameters as the DeepONet. Both models are optimized using the Adam optimizer [14] with a learning rate of 0.001 on identical datasets.

The code is conducted using PyTorch [28] and MATLAB 2019b on a workstation with Nvidia GTX 1080Ti graphics card, and an Intel Core i5-7500 processor, 16 GB RAM. It is noteworthy that the evaluation of time complexity is based on the Performance function (PF) calls N_{call} , which refers to the number of system simulations that need to be executed, rather than the program's running time, as program running speeds may vary significantly across different programming languages and platforms. The PF calls consist of the evaluation of hybrid algorithm in line 6 of Algorithm 2.1 and simulations for generating training data in (3.5). It should also be noted that the hierarchical neural hybrid [18, 35] approach only reduces program running time, but not the PF calls. We do not evaluate the computational time required for the neural surrogate or the neural operator surrogate, as a trained model using batch techniques can evaluate 10^5 samples in less than a second.

4.1. Ordinary differential equation. In this test problem, we consider a random ordinary differential equation (ODE) proposed in [17]. The ODE is given by:

$$(4.1) \quad \frac{ds}{dt} = -Zs, \quad s(0) = s_0,$$

where $s_0 = 1$, and $Z \sim \mathcal{N}(\mu, \sigma^2)$ is a Gaussian random variable with mean $\mu = -2$ and standard deviation $\sigma = 1$. The limit state function is defined as $g(Z) = g(s(t, Z)) = s(t, Z) - s_d$, where $s_d = 0.5$ and $t = 1$. The exact failure probability $P_f = 0.003539$ is regarded as the reference solution, which can be computed using the analytic solution $s(t, Z) = s_0 e^{-Zt}$.

To demonstrate the efficiency and effectiveness of the proposed NOH method, we compare it with the Monte Carlo simulation (MCS) and the NH method. We use DeepONet to train the neural operator surrogate in the NOH method and set the parameter k in (3.10) to 4, the number of input functions for training N to 500, and the number of sensors m to 100. In the NH method, we use the FNN as the neural surrogate.

Both surrogates in the NH and NOH method are trained using identical datasets, epochs, and optimizers. Additionally, in the MCS, 10^6 samples are generated to estimate the failure probability.

Table 1: Comparison of Monte Carlo simulation (MCS), the Neural Hybrid (NH) method and the Neural Operator Hybrid (NOH) method. In the hybrid algorithm, we set δM to 25, ϵ to 0, and terminate the iterative procedure when $\delta P \leq \epsilon$ for 5 times.

Method	P_f^h	N_{call}	ϵ_e
MCS	3.578×10^{-3}	10^6	0.11%
NOH	3.578×10^{-3}	500(Training)+ 1750(Evaluating)	0.11%
NH	-	-	-

Table 1 presents the performance of the MCS, the NOH method and the NH method. As shown in the table, the NOH method outperforms MCS by achieving the same level of estimation precision with only approximately $O(N_{call}/1000)$ or 0.23% of the PF calls required by MCS. The NH method fails to estimate the failure probability, as all the outputs of the neural surrogate are greater than 0. In this special case, the hybrid iterative procedure always terminates too early, while the estimated failure probability remains at 0.

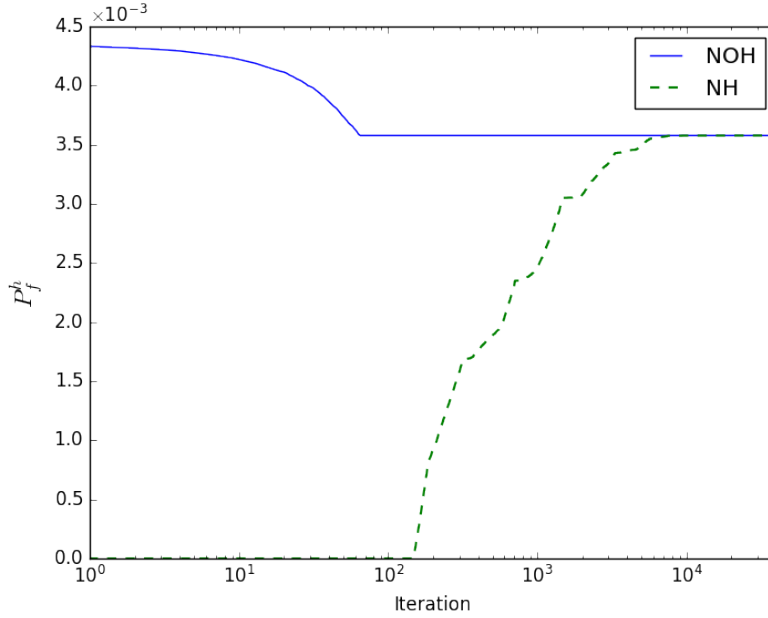


Fig. 2: Convergence of the NOH method and the NH method. In the hybrid algorithm, we set δM to 25, and the iterative procedure is not terminated until the limit state function g is recomputed for 10^4 iterations.

Figure 2 illustrates the convergence of the NOH method and the NH method. In order to compare the two methods, the iterative procedure in the hybrid algorithm

is not terminated until the limit state function g is recomputed for at least 10^5 samples. The figure shows that the estimate of the failure probability by the NH method remains at 0 until around 100 iterations, and it converges after approximately 7000 iterations. In contrast, the NOH method converges after only 70 iterations, demonstrating its superior efficiency compared to the NH method.

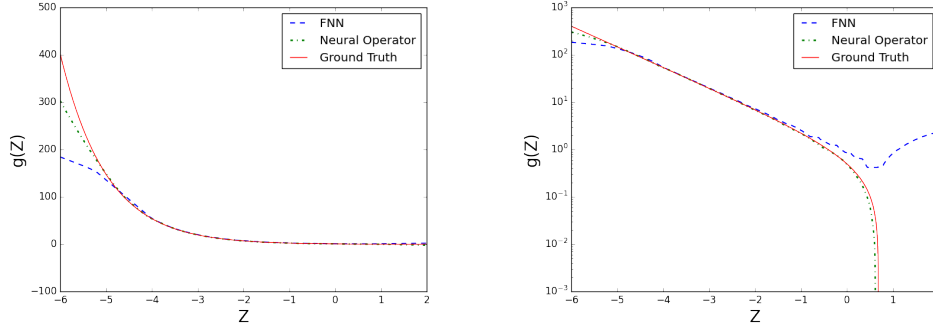


Fig. 3: Comparison of the neural surrogate and the neural operator surrogate.

In Figure 3, we compare the performance of the neural surrogate and the neural operator surrogate for predicting the limit state function g . We observed that all the outputs of the neural surrogate are greater than zero, which leads to the failure of the NH method for estimating the failure probability. It is evident that the neural operator surrogate outperforms the neural surrogate in predicting the limit state function g .

4.2. Multivariate benchmark. Next, we consider a high-dimensional multivariate benchmark problem (the dimensionality $n = 50$) in the field of structural safety in [18, 9].

$$(4.2) \quad g(Z) = \beta n^{\frac{1}{2}} - \sum_{i=1}^n Z_i,$$

where $\beta = 3.5$ and each random variable $Z_i \sim \mathcal{N}(0, 1)$, $i = 1, \dots, n$. $g(Z)$ is the limit state function. In this test problem, the reference failure probability is $P_f^{mc} = 2.218 \times 10^{-4}$, which is obtained by MCS with 5×10^6 samples.

The proposed NOH method is compared with the NH method in terms of accuracy and efficiency. For the NOH method, we set the parameter k in (3.10) to 4, the number of input functions N to 1000, and the number of sensors m to 100. In comparison, a naive FNN surrogate with a similar number of parameters was also constructed for NH method, and trained under identical conditions.

The performance of the MCS, the NOH method, and the NH method are illustrated in Table 2. It can be observed that the NOH method requires fewer N_{call} compared to the MCS and the NH method, while still providing failure probability estimates that are consistent with the reference failure probability (estimated by the MCS).

Table 2: The performance evaluation was conducted to compare the MCS, the NH, and the NOH approaches. The NOH method was found to outperform the other methods. Specifically, the NOH method achieved best relative error of 0.81%, while requiring the least number of samples compared to the other methods.

Method	P_f^h	N_{call}	ϵ_e
MCS	2.22×10^{-4}	10^6	-
NOH	2.20×10^{-4}	1000 (Training) + 150 (Evaluating)	0.81%
NH	2.02×10^{-4}	1000 (Training) + 4175 (Evaluating)	8.92 %

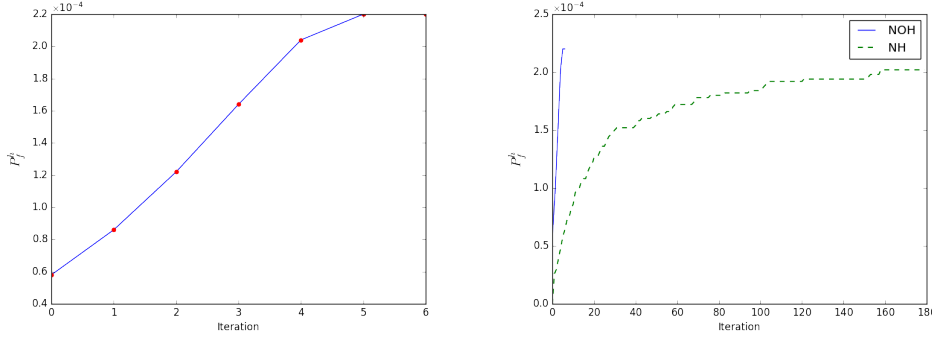


Fig. 4: Convergence of the NOH method and the NH method. The left figure demonstrates the convergence of the NOH method, while in the other a comparison of the convergence rates between the NOH and the NH methods was conducted, with $\delta M = 25$ in each iteration. NOH converges obviously much faster than NH, which indicates much more precise in approximation.

The convergence of the NOH method is depicted and compared with the NH method in Figure 4. The NOH method achieves an estimation of $P_f^h = 2.2 \times 10^{-4}$ with a relative error $\epsilon_e = 0.81\%$ in less than six iterations. Despite requiring significantly fewer samples compared to the MCS, both the NOH method and the NH method exhibit faster convergence rates. Moreover, the NOH method is observed to converge much faster than the NH method, suggesting that it is more precise in its approximation. These findings highlight the efficiency of the operator learning scheme used in the NOH method.

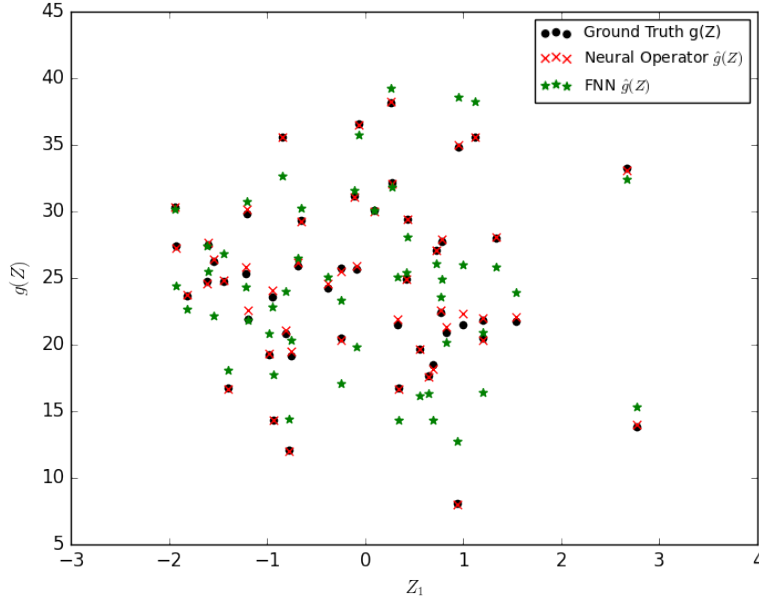


Fig. 5: Comparison of the neural surrogate and the neural operator surrogate by using 50 randomly selected samples. The figure demonstrate the error projected onto Z_1 .

Figure 5 depicts a comparison between the approximations obtained by the neural surrogate and the neural operator surrogate for 50 randomly selected samples. As illustrated in the figure, the predictions of the limit function g by the neural operator surrogate, are more accurate compared to the neural surrogate, as the former closely approximates the ground truth.

4.3. Helmholtz Equation. We consider the Helmholtz equation on a disk with a square Hole [18]. The equation is given by:

$$(4.3) \quad -\Delta u - \kappa^2 u = 0,$$

where coefficient κ is a Gaussian random variable with mean $\mu = 60$, and variance $\sigma = 1$, i.e., $\kappa \sim \mathcal{N}(60, 1)$. The system is set with a homogeneous term, and Dirichlet boundary conditions ($u = 0$) are applied on the edges of the square hole, while generalized Neumann conditions ($\vec{\xi} \cdot \nabla r - i\kappa r = 0$ here $\vec{\xi}$ is the radial distance from the object) are applied on the edge of the disk. The system is numerically solved using the MATLAB PDE solver to obtain an accurate solution. A snapshot of the solution of Helmholtz is shown in Figure 6. A point sensor is placed at $x_p = [0.7264; 0.4912]$, and the failure probability is defined as $\text{Prob}(u(x_p, \kappa) > 1.00)$. The reference solution is $P_f^{mc} = 2.70 \times 10^{-4}$, obtained by Monte Carlo simulation with 10^5 samples.

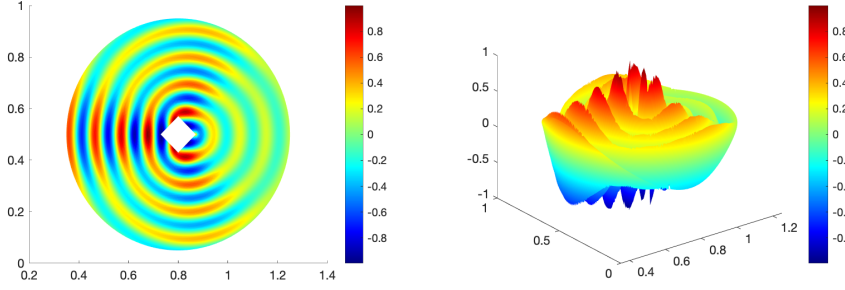


Fig. 6: A snapshot of the solution of Helmholtz equation.

Following a setup similar to the previous experiment, we use DeepONet to train the neural operator surrogate in the NOH method and set the parameter k in (3.10) to 4, the number of input functions N to 1000, and the number of sensors m to 100. We use the fully connected neural network (FNN) as the neural surrogate in the NH method, and trained both model under identical conditions.

Table 3: The performance evaluation was conducted to compare the NH and the NOH approaches. The NOH method was found to outperform the NH method. Specifically, the NOH method achieved a relative error of just 3.70%, while requiring fewer samples compared to the NH method.

Method	P_f^h	N_{call}	ϵ_e
MCS	2.70×10^{-4}	10^5	-
NOH	2.80×10^{-4}	1000 (Training) + 100 (Evaluating)	3.70%
NH	3.00×10^{-4}	1000 (Training) + 875 (Evaluating)	11.11%

We present the performance analysis of the Monte Carlo simulation (MCS), the NOH method, and the NH method in Table 3. The results indicate that the NOH method requires fewer N_{call} compared to the NH method, while providing a more accurate estimate of the failure probability. This highlights the efficiency and accuracy of the NOH method compared to the NH method.

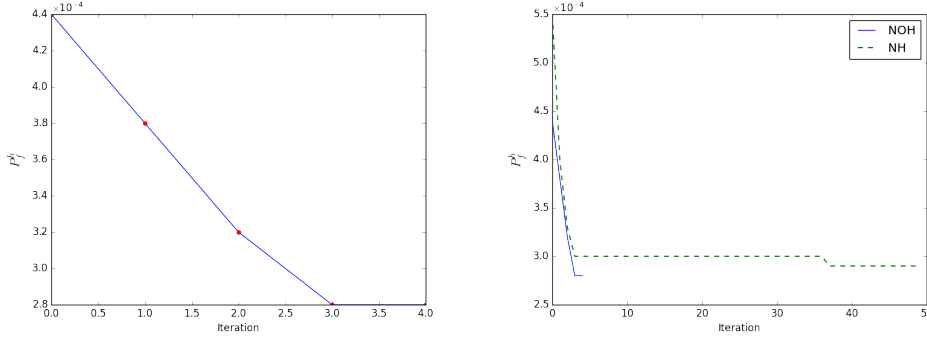


Fig. 7: Convergence of the NOH method and the NH method. The left figure demonstrates the convergence of the NOH method, while in the other a comparison of the convergence rates between the NOH and the NH methods was conducted, with $\delta M = 25$ in each iteration.

The convergence of the NOH method is illustrated and compared with NH method in Figure 7. Both methods converge quickly, but the NOH method outperforms the NH method in terms of accuracy. With only 100 evaluation samples, the NOH method can accurately estimate the failure probability as $P_f^h = 2.80 \times 10^{-4}$, with a relative error of 3.70% compared to the MCS estimation.

On the other hand, the NH method, which employs an FNN neural surrogate, performed significantly worse, possibly due to the lack of precision of FNN, causing the iterative procedure to terminate early. Despite using 875 evaluations, the NH method only provided a less accurate estimate, i.e., $P_f^h = 3.00 \times 10^{-4}$, with a higher relative error of 11.11%. These results demonstrate that the NOH method outperforms the NH method in both accuracy and efficiency.

5. Conclusions. This paper introduces a neural operator hybrid method for the estimation of the failure probability. Instead of approximating the limit state function directly, we reframe the problem as an operator learning task. This allows us to construct a highly efficient and precise surrogate operator model, which can accurately estimate the limit state function. By integrating the surrogate operator model into the hybrid algorithm, we achieve the neural operator hybrid method. Our numerical results demonstrate that the proposed method provides an efficient strategy for estimating failure probability, particularly in systems governed by ODE, multivariate function, and the Helmholtz equation. These results suggest that neural operator learning holds significant potential for failure probability estimation, and we will explore the expansion of neural operator learning in our future work.

REFERENCES

- [1] P. BJERAGER, *Probability integration by directional simulation*, Journal of Engineering Mechanics, 114 (1988), pp. 1285–1302.
- [2] S. BOYAVAL, C. L. BRIS, T. LELIÈVRE, Y. MADAY, N. C. NGUYEN, AND A. T. PATERA, *Reduced basis techniques for stochastic problems*, Archives of Computational Methods in Engineering, 4 (2010), pp. 435–454, <https://doi.org/10.1007/s11831-010-9056-z>.

- [3] S. CAI, Z. WANG, L. LU, T. A. ZAKI, AND G. E. KARNIADAKIS, *Deepm&mnet: Inferring the electroconvection multiphysics fields based on operator approximation by neural networks*, Journal of Computational Physics, 436 (2021), p. 110296.
- [4] T. CHEN AND H. CHEN, *Approximations of continuous functionals by neural networks with application to dynamic systems*, IEEE Transactions on Neural networks, 4 (1993), pp. 910–918.
- [5] T. CHEN AND H. CHEN, *Approximation capability to functions of several variables, nonlinear functionals, and operators by radial basis function neural networks*, IEEE Transactions on Neural Networks, 6 (1995), pp. 904–910.
- [6] G. CYBENKO, *Approximation by superpositions of a sigmoidal function*, Mathematics of control, signals and systems, 2 (1989), pp. 303–314.
- [7] A. DER KIUREGHIAN AND T. DAKESSIAN, *Multiple design points in first and second-order reliability*, Structural Safety, 20 (1998), pp. 37–49.
- [8] O. DITLEVSEN AND P. BJERAGER, *Methods of structural systems reliability*, Structural Safety, 3 (1986), pp. 195–229.
- [9] S. ENGELUND AND R. RACKWITZ, *A benchmark study on importance sampling techniques in structural reliability*, Structural Safety, 12 (1993), pp. 255–276, [https://doi.org/https://doi.org/10.1016/0167-4730\(93\)90056-7](https://doi.org/https://doi.org/10.1016/0167-4730(93)90056-7), <https://www.sciencedirect.com/science/article/pii/0167473093900567>.
- [10] R. G. GHANEM AND P. D. SPANOS, *Stochastic finite elements: a spectral approach*, Courier Corporation, 2003.
- [11] M. HOHENBICHLER, S. GOLLWITZER, W. KRUSE, AND R. RACKWITZ, *New light on first-and second-order reliability methods*, Structural safety, 4 (1987), pp. 267–284.
- [12] K. HORNIK, M. STINCHCOMBE, AND H. WHITE, *Multilayer feedforward networks are universal approximators*, Neural networks, 2 (1989), pp. 359–366.
- [13] A. I. KHURI AND S. MUKHOPADHYAY, *Response surface methodology*, Wiley Interdisciplinary Reviews: Computational Statistics, 2 (2010), pp. 128–149.
- [14] D. P. KINGMA AND J. BA, *Adam: A method for stochastic optimization*, arXiv preprint arXiv:1412.6980, (2014).
- [15] M. KUTYŁOWSKA, *Neural network approach for failure rate prediction*, Engineering Failure Analysis, 47 (2015), pp. 41–48.
- [16] J. LI, J. LI, AND D. XIU, *An efficient surrogate-based method for computing rare failure probability*, Journal of Computational Physics, 230 (2011), pp. 8683–8697, <https://doi.org/10.1016/j.jcp.2011.08.008>, <http://dx.doi.org/10.1016/j.jcp.2011.08.008>.
- [17] J. LI AND D. XIU, *Evaluation of failure probability via surrogate models*, Journal of Computational Physics, 229 (2010), pp. 8966–8980, <https://doi.org/10.1016/j.jcp.2010.08.022>, <http://dx.doi.org/10.1016/j.jcp.2010.08.022>.
- [18] K. LI, K. TANG, J. LI, T. WU, AND Q. LIAO, *A hierarchical neural hybrid method for failure probability estimation*, IEEE Access, 7 (2019), pp. 112087–112096, <https://doi.org/10.1109/ACCESS.2019.2934980>, <https://arxiv.org/abs/1908.01235>.
- [19] Z. LI, N. KOVACHKI, K. AZIZZADENESHELI, B. LIU, K. BHATTACHARYA, A. STUART, AND A. ANANDKUMAR, *Fourier neural operator for parametric partial differential equations*, arXiv preprint arXiv:2010.08895, (2020).
- [20] Q. X. LIEU, K. T. NGUYEN, K. D. DANG, S. LEE, J. KANG, AND J. LEE, *An adaptive surrogate model to structural reliability analysis using deep neural network*, Expert Systems with Applications, 189 (2022), p. 116104, <https://doi.org/10.1016/j.eswa.2021.116104>, <https://doi.org/10.1016/j.eswa.2021.116104>.
- [21] C. LIN, Z. LI, L. LU, S. CAI, M. MAXEY, AND G. E. KARNIADAKIS, *Operator learning for predicting multiscale bubble growth dynamics*, The Journal of Chemical Physics, 154 (2021), p. 104118.
- [22] L. LU, P. JIN, G. PANG, Z. ZHANG, AND G. E. KARNIADAKIS, *Learning nonlinear operators via DeepONet based on the universal approximation theorem of operators*, Nature Machine Intelligence, 3 (2021), pp. 218–229, <https://doi.org/10.1038/s42256-021-00302-5>, <https://arxiv.org/abs/arXiv:1910.03193v3>.
- [23] L. LU, X. MENG, S. CAI, Z. MAO, S. GOSWAMI, Z. ZHANG, AND G. E. KARNIADAKIS, *A comprehensive and fair comparison of two neural operators (with practical extensions) based on FAIR data*, Computer Methods in Applied Mechanics and Engineering, 393 (2022), pp. 1–42, <https://doi.org/10.1016/j.cma.2022.114778>, <https://arxiv.org/abs/2111.05512>.
- [24] L. LU, X. MENG, Z. MAO, AND G. E. KARNIADAKIS, *Deepxde: A deep learning library for solving differential equations*, SIAM review, 63 (2021), pp. 208–228.
- [25] Z. MAO, L. LU, O. MARXEN, T. A. ZAKI, AND G. E. KARNIADAKIS, *Deepm&mnet for hypersonics: Predicting the coupled flow and finite-rate chemistry behind a normal shock using*

- neural-network approximation of operators*, Journal of computational physics, 447 (2021), p. 110698.
- [26] G. PANG, L. LU, AND G. E. KARNIADAKIS, *fpinns: Fractional physics-informed neural networks*, SIAM Journal on Scientific Computing, 41 (2019), pp. A2603–A2626.
 - [27] M. PAPADRAKAKIS AND N. D. LAGAROS, *Reliability-based structural optimization using neural networks and monte carlo simulation*, Computer methods in applied mechanics and engineering, 191 (2002), pp. 3491–3507.
 - [28] A. PASZKE, S. GROSS, F. MASSA, A. LERER, J. BRADBURY, G. CHANAN, T. KILLEEN, Z. LIN, N. GIMELSHEIN, L. ANTIGA, A. DESMAISON, A. KÖPF, E. Z. YANG, Z. DEVITO, M. RAISON, A. TEJANI, S. CHILAMKURTHY, B. STEINER, L. FANG, J. BAI, AND S. CHINTALA, *Pytorch: An imperative style, high-performance deep learning library*, CoRR, abs/1912.01703 (2019), <http://arxiv.org/abs/1912.01703>, <https://arxiv.org/abs/1912.01703>.
 - [29] A. QUATERONI, A. MANZONI, AND F. NEGRI, *Reduced basis methods for partial differential equations: An introduction*, Springer, 2016.
 - [30] M. RAISSI, P. PERDIKARIS, AND G. E. KARNIADAKIS, *Physics-informed neural networks: A deep learning framework for solving forward and inverse problems involving nonlinear partial differential equations*, Journal of Computational physics, 378 (2019), pp. 686–707.
 - [31] M. R. RAJASHEKHAR AND B. R. ELLINGWOOD, *A new look at the response surface approach for reliability analysis*, Structural safety, 12 (1993), pp. 205–220.
 - [32] A. TABANDEH, G. JIA, AND P. GARDONI, *A review and assessment of importance sampling methods for reliability analysis*, Structural Safety, 97 (2022), p. 102216, <https://doi.org/10.1016/j.strusafe.2022.102216>, <https://doi.org/10.1016/j.strusafe.2022.102216>.
 - [33] R. TEIXEIRA, M. NOGAL, AND A. O’CONNOR, *Adaptive approaches in metamodel-based reliability analysis: A review*, Structural Safety, 89 (2021), p. 102019, <https://doi.org/10.1016/j.strusafe.2020.102019>, <https://doi.org/10.1016/j.strusafe.2020.102019>.
 - [34] D. XIU AND G. E. KARNIADAKIS, *The Wiener-Askey polynomial chaos for stochastic differential equations*, SIAM journal on scientific computing, 24 (2002), pp. 619–644, <https://doi.org/10.1137/S1064827501387826>.
 - [35] C. YAO, J. MEI, AND K. LI, *A mixed residual hybrid method for failure probability estimation*, in 2022 17th International Conference on Control, Automation, Robotics and Vision (ICARCV), IEEE, 2022, pp. 119–124.
 - [36] D. ZHANG, L. GUO, AND G. E. KARNIADAKIS, *Learning in modal space: Solving time-dependent stochastic pdes using physics-informed neural networks*, SIAM Journal on Scientific Computing, 42 (2020), pp. A639–A665.